Tellus SERIES B CHEMICAL AND PHYSICAL METEOROLOGY
PUBLISHED BY THE INTERNATIONAL METEOROLOGICAL INSTITUTE IN STOCKHOLM

Tellus (2008), 60B, 569–582
Printed in Singapore. All rights reserved

TELLUS

Vertical profiles and storage fluxes of CO_2, heat and water in a tropical rainforest at Pasoh, Peninsular Malaysia

By SHINJIRO OHKUBO[1]*, YOSHIKO KOSUGI[1], SATORU TAKANASHI[2], NAOKO MATSUO[3], MAKOTO TANI[1] and ABDUL RAHIM NIK[4], [1]*Graduate School of Agriculture, Kyoto University, Kyoto 606-8502, Japan;* [2]*Forestry and Forest Products Research Institute, Tsukuba, Ibaraki 305-8687, Japan;* [3]*Faculty of Bioresources, Mie University, Tsu, Mie 514-8507, Japan;* [4]*Forest Research Institute Malaysia, Kepong, Kuala Lumpur 52109, Malaysia*

(Manuscript received 8 November 2007; in final form 27 April 2008)

ABSTRACT

Ambient CO_2 concentration, air temperature and relative humidity were measured intermittently for a 3-year period from the floor to the canopy top of a tropical rainforest in Pasoh, Peninsular Malaysia. Mean diurnal CO_2 storage flux (S_c; μmol m^{-2} s^{-1}) and sensible and latent heat storage fluxes (Q_a and Q_w; W m^{-2}) ranged from -12.7 to 3.2 μmol m^{-2} s^{-1}, -15 to 27 W m^{-2} and -10 to 20 W m^{-2}, respectively. Small differences in diurnal changes were observed in S_c and Q_a between the driest and wettest periods. Compared with the ranges of mean diurnal CO_2 eddy flux (-14.7 to 4.9 μmol m^{-2} s^{-1}), sensible eddy flux (-12 to 169 W m^{-2}) and latent eddy flux (0 to 250 W m^{-2}), the contribution of CO_2 storage flux was especially large. Comparison with summertime data from a temperate Japanese cypress forest suggested a higher contribution of S_c in the tropical rainforest, probably mainly due to the difference in nighttime friction velocity at the sites. On the other hand, differences in Q_a and Q_w were smaller than the difference in S_c, probably because of the smaller nighttime sinks/sources of heat and water vapour.

1. Introduction

Globally, the most important interactions between terrestrial ecosystems and the atmosphere include energy, water and carbon transfers. The magnitudes of these exchange processes vary with climate and vegetation. Eddy covariance is one of the best meteorological methods for evaluating CO_2 and energy exchanges between forests and the atmosphere. However, this method has been widely reported as unreliable for estimating CO_2 exchange between forests and the atmosphere at night (e.g. Law et al., 1999; Baldocchi, 2003). Eddy covariance generally underestimates nighttime CO_2 emission from forests (i.e. ecosystem respiration). Energy exchange imbalance has also been reported at many forest sites (Wilson et al., 2002). To overcome these problems, we must clarify the processes of CO_2 and energy exchanges between forests and the atmosphere. Generally, CO_2 and energy exchanges between a forest and the atmosphere consist of three components: eddy flux; storage flux and mass flow—arising from horizontal flow convergence/divergence or a non-zero mean vertical velocity at the observation height (e.g. Lee, 1998). Recently, horizontal and vertical advective CO_2 fluxes have been estimated by observing wind speed and CO_2 concentration spatially at many points with numerous instruments (Sun et al., 2007; Feigenwinter et al., 2008). They showed the characteristics of the advective CO_2 fluxes and indicated that the contributions of advective fluxes to CO_2 exchange were not negligible, although detailed investigations are needed for more accurate estimation. Storage fluxes of CO_2, sensible heat and latent heat also cannot be ignored, especially for closed forests with a tall canopy. In the absence of advection, the daily net storage of CO_2, sensible heat and latent heat in the air column should be roughly zero. Over the course of a day or more, stored CO_2, sensible heat and latent heat change very little; however, under some conditions, large contributions of these storage fluxes may occur over shorter time scales and should be evaluated to assess their contributions to eddy fluxes. Within the air space of such a forest, the meteorological environment varies from the floor to

*Corresponding author.
e-mail: shinjiro@kais.kyoto-u.ac.jp
DOI: 10.1111/j.1600-0889.2008.00367.x

the canopy top, and vertical profiling is a very important method for evaluating storage fluxes and understanding the process of gas exchange.

By measuring the CO_2 concentration ($[CO_2]$) at several heights, vertical concentration (μmol m^{-3}) profiles and CO_2 storage flux (S_c; μmol m^{-2} s^{-1}) estimates have been made for a number of forest types (e.g. Brooks et al., 1997; Jarvis et al., 1997; Hollinger et al., 1998; Malhi et al., 1998; Dolman et al., 2002; Kondo et al., 2005; Ohkubo et al., 2007). Similarly, by measuring the air temperature and relative humidity at several heights, sensible and latent heat storage flux (Q_a and Q_w, respectively; W m^{-2}) estimates have been made in a several kinds of forests (e.g. McCaughey and Saxton, 1988; Vogt et al., 1996; Silberstein et al., 2001; Turnipseed et al., 2002; Oliphant et al., 2004).

A great deal of gas exchange is thought to occur in tropical rainforests. Despite the importance of such exchanges, however, few studies have continuously measured the stored CO_2, sensible heat and latent heat fluxes in tropical rainforests, coupled with eddy flux measurements above the canopy. Massive stores of CO_2, heat and water are thought to exist in tropical rainforests due to the warm temperature, generous year-round incoming radiation and large quantity of biomass. Moreover, tropical rainforests are structurally complex, with tall canopies, and their environmental factors vary from the forest floor to canopy top. Thus, much more information is needed to understand the exchange of CO_2, sensible heat and latent heat within the tropical region. Previous studies of storage fluxes in Southeast Asian tropical rainforests have mainly relied on short-term measurements collected at only two sites: Lambir Hills National Park in Sarawak, Malaysia (H_c, 50–60 m; leaf area index, LAI, 5.1) and the Pasoh Forest Reserve (PSO) in Peninsular Malaysia (H_c, 35–45 m; LAI, 6.52). Kumagai et al. (2001) described the micrometeorological conditions in a forest canopy at Lambir Hills National Park, using measurements of several environmental factors, including global solar radiation, wind speed, air temperature, humidity and $[CO_2]$ above and within the canopy, which were collected for a week. Similarly, in PSO, Aoki et al. (1975) measured environmental factors over a several-day period to study the micrometeorology and primary production of the forest, whereas Yasuda et al. (2003) used data collected over a 3-d period to produce a six-level $[CO_2]$ profile to estimate CO_2 storage flux and net ecosystem exchange (NEE). Clearly, long-term observation of these storage parameters is needed to understand the process of each element's formation under various conditions.

In this study, we profiled $[CO_2]$, air temperature and relative humidity at 8 or 10 heights intermittently for 2 or 3 yr, concomitantly with eddy covariance measurements over the canopy to clarify the diurnal and seasonal patterns of vertical profiles and storage fluxes, changes in the storage fluxes under various meteorological conditions and the contribution of the storage fluxes to CO_2 and energy exchanges.

2. Materials and methods

2.1. Site description

The study site is located in the PSO near Simpang Pertang at Negri Sembilan in Peninsular Malaysia (2°58′N, 102°18′E). The core area (600 ha) of the reserve (2450 ha) is covered with a primary lowland mixed dipterocarp forest (tropical evergreen broadleaved forest) that includes various species of *Shorea* and *Dipterocarpus*. The continuous canopy height is approximately 35 m, although some emergent trees exceed 45 m. The LAI, estimated from tree-diameter measurements (Niiyama, unpublished), is 6.52. The topography in the forest is gently undulating. There are two rainy seasons in the region (March–May and October–December), brought by the southwestern and northeastern monsoons, respectively. Seasonal rainfall fluctuations have been described by Noguchi et al. (2003) and Kosugi et al. (2008). From 2003 to 2005, the average annual air temperature at 52 m was 26.2 °C and the mean annual precipitation was 1739 mm.

2.2. Measurements

Eddy fluxes of CO_2, sensible heat and latent heat were measured by the eddy covariance method at a height of 54 m from an observation tower. The wind speed and temperature were measured with a three-axis sonic anemometer (SAT-550, Kaijo, Tokyo, Japan), and the concentrations of CO_2 and H_2O were monitored with an open-path infrared gas analyzer (IRGA; LI-7500, LI-COR, Inc., Lincoln, NE, USA). The data were sampled at 10 Hz and sent to a data logger (CR-5000, Campbell Scientific, Logan, UT, USA). Detailed descriptions of the eddy covariance measurements have been provided by Kosugi et al. (2008). Downward short-wave radiation was monitored from the observation tower at a height of 52 m (MR22, EKO, Tokyo, Japan). Soil water contents at depths of 0.1, 0.2 and 0.3 m (CS515, Campbell Scientific) were monitored with nine sensors at three points around the tower. Vertical profiles of air temperature and relative humidity were made at eight levels (1, 5, 10, 20, 30, 40, 45 and 53 m) using ventilated temperature and relative humidity sensors (HMP45A and HMP45C, Vaisala, Boulder, CO, USA). The air temperature and relative humidity at the site have been under continuous observation since March 2003. Other meteorological observations, described by Kosugi et al. (2008), were logged every 10 min using three data loggers (CR-10X, Campbell Scientific).

We used an IRGA and an automated profiling system (HT-CT-P; Hydrotech, Shiga, Japan) to produce the $[CO_2]$ profile. Air samples for $[CO_2]$ measurement were drawn continuously at a flow rate of 2000 ml min^{-1} through a 4-mm internal diameter polyethylene tube at each inlet from ten levels (0.2, 0.5, 1, 2, 5, 10, 20, 30, 45 and 53 m) by a closed-path IRGA (LI-7000, LI-COR, Inc.). The IRGA was located in an observation house

on the forest floor. The profile system sampled an entire profile every 5 min. Depending on the measuring height, 12 to 35 s were allowed to flush the tubing of residual air before sampling with the IRGA. We selected the purging time based on a pulse test of high-concentration CO_2 through a tube. The IRGA was automatically calibrated daily, using zero concentration gas (N_2). We conducted continuous short-term [CO_2] profile measurements several times a year for terms of several weeks to 1 month. We replaced the IRGA after every observation term and checked the zero and span of CO_2 at the beginning and end of each observation term. Data collected when a serious gap in zero was observed were excluded. In every case, the span was quite stable. Switching between the canopy heights was controlled by a control port module (SDM-CD16AC, Campbell Scientific) and a series of solenoid valves (FAG31-6-4-12C, CKD, Rolling Meadows, IL, USA). The [CO_2] was recorded by a data logger (CR-23X, Campbell Scientific). The basic principles of the profiling system for CO_2 and its accuracy are described in detail in Xu et al. (1999) and Mölder et al. (2000), although some minor parts of their measurement systems are different from ours. The CO_2 profile was measured intermittently from September 2004 to November 2005, a period that included rainy and dry seasons. Occasional system breakdown or trouble with the sensors, mainly caused by thunder, limited the completeness of the profile data available for calculating the storage terms.

2.3. Calculations

Eddy fluxes of CO_2 (F_c, μmol m^{-2} s^{-1}), sensible heat ($\boldsymbol{H}$, W m^{-2}) and latent heat ($\lambda\boldsymbol{E}$, W m^{-2}) over the canopy were calculated with an averaging time of 30 min. The F_c, $\boldsymbol{H}$ and $\lambda\boldsymbol{E}$ in this study showed the eddy covariance fluxes measured over the canopy, not including the storage fluxes. A Webb, Penman and Leuning (WPL) correction for the effect of air density fluctuations (Webb et al., 1980) was applied. Linear trends in temperature, water vapour and CO_2 concentration were not removed, as linear de-trending might cause underestimates of low-frequency flux, which is thought to be large for tall tropical forests with low wind speeds, low turbulent intensity, and thus, large eddies that can transport flux. The influence of linear de-trending can also be assessed by considering the annual integration of CO_2 exchange (Kosugi et al., 2008). Comparison of averaging times of 1 h and 30 min showed that the contribution of the larger scale component was approximately 2.0% (n = 12 094, median; 1-h F_c data were compared with the average of 30-min F_c for 1 h, for data from 2002 to 2005). Although this difference should be accounted for, we used 30 min for the averaging time, because with a 1-h averaging time, a stationarity check showed too many data of poor quality (Kosugi et al., 2008).

The storage fluxes (S_c, Q_a and Q_w) were calculated from the following equations:

$$S_c = \int_0^{Z_r} \left(\frac{\delta c}{\delta t}\right) \mathrm{d}z \tag{1}$$

where Z_r, c, t and z represent the height of the eddy flux measurement (m), the [CO_2], the time (s) and the height from the ground (m), respectively. Considering the time from each inlet to the IRGA, we used data from the last 11 s of each cycle. We collected data six times and calculated the average at each height every 30 min:

$$Q_a = \int_0^{Z_r} \rho C_p \left(\frac{\delta T_a}{\delta t}\right) \mathrm{d}z \tag{2}$$

where ρ, C_p and T_a are the air density (kg m^{-3}), specific heat (J kg^{-1} K^{-1}) and air temperature (K), respectively. We calculated the average T_a every 30 min. The storage flux Q_w was given by

$$Q_w = \int_0^{Z_r} \left(\frac{\rho C_p}{\Gamma}\right)\left(\frac{\delta e}{\delta t}\right) \mathrm{d}z \tag{3}$$

where Γ and e are the psychrometric constant (hPa K^{-1}) and water vapour pressure (hPa), respectively. The values of $\delta c/\delta t$, $\delta T_a/\delta t$ and $\delta e/\delta t$ were calculated by dividing 30 min into the difference in 30-min mean c, T_a and e between the beginning and end of each 30-min run. We assumed that c, T_a and e varied linearly between the measurement points. Finally, we determined each storage flux by calculating $\delta c/\delta t$, $\delta T_a/\delta t$ and $\delta e/\delta t$ from the differences between the averaged values for c, T_a and e, respectively, every 30 min. A previous study estimated that the biomass heat storage in the study forest ranges from -10 to 15 W m^{-2} based on short-term stem temperature and heat-plate measurements. Lamaud et al. (2001) reported that the energy fixed by photosynthesis represents only 1–3% of the incident net radiation at the canopy scale. Although these terms can sometimes be significant, we did not deal with them in this study.

Recently, Finnigan (2006) showed that for accuracy, the storage flux should be calculated using the difference between the volume mean scalar at the beginning and end of each run. To assess the difference between the two methods, we also calculated CO_2 concentration at each height every 5 and 15 min and calculated CO_2 storage fluxes (S_{c5} and S_{c15}, μmol m^{-2} s^{-1}) every 30 min by averaging the results of six and two runs, respectively. We also compared these storage fluxes (S_{c5} and S_{c15}) with S_c (Fig. 1). The data were divided by u_*. The relationships between S_c and S_{c5} and S_{c15} seem to be approximately 1:1, although some dispersion was observed. In addition, open circles representing high u_* seemed to be concentrated near the 1:1 lines. Large differences between S_c and S_{c5} and S_{c15} were seen when S_c was large and u_* was small during nighttime (data not shown). The indices of dispersion $\frac{\sum(S_c-S_{c5})^2}{N}$ and $\frac{\sum(S_c-S_{c15})^2}{N}$ (N is the number of data) were 45.2 and 28.4 with small u_* (<0.4 m s^{-1}) and 9.7 and 4.8 with large u_* ($\geq$0.4 m s^{-1}), respectively. These values indicate that data averaged over a short time might be influenced by horizontal heterogeneity in the CO_2 concentration; strong air mixing decreases the heterogeneity. In this study, we adopted a 30-min averaging time because short-time-averaged data might be biased by a single gust. For the period from 0:00 to 0:30, we averaged the [CO_2] data from 0:05 to 0:30, because the IRGA

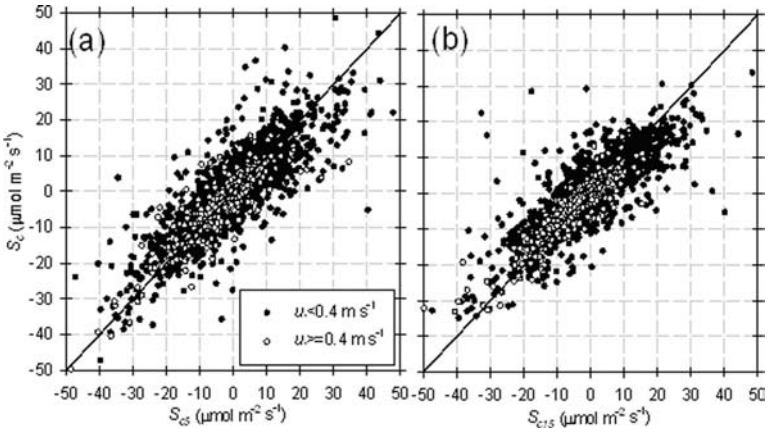

Fig. 1. Relationship between S_c and S_{c5} (a) and S_{c15} (b). We classified the data as small u_* (<0.4 m s^{-1}; solid circles) and large u_* (≥0.4 m s^{-1}; open circles). The lines indicate a 1:1 relationship.

Table 1. The ratio of the number of available 30-min data to the whole period for each month for S_c and Q_a and Q_w (%)

		Jan	Feb	Mar	Apr	May	Jun	Jul	Aug	Sep	Oct	Nov	Dec
2003	S_c	–	–	–	–	–	–	–	–	–	–	–	–
	Q_a, Q_w	–	–	–	–	–	–	–	30	100	61	–	48
2004	S_c	–	–	–	–	–	–	–	–	21	90	28	100
	Q_a, Q_w	100	100	40	34	100	79	–	–	–	–	–	–
2005	S_c	40	48	72	–	–	21	8	–	–	42	25	–
	Q_a, Q_w	–	–	–	–	–	–	98	100	98	62	73	–

was calibrated from 0:00 to 0:05 every day. Table 1 shows the ratio of the number of available 30-min data points to the whole period for each month.

We compared the data from this study with results from the Kiryu Experimental Watershed in a temperate Japanese cypress forest in Shiga Prefecture, Japan (34°58′N, 136°00′E). From 2004 to 2006, the Kiryu site had an average annual air temperature of 13.3 °C and mean annual precipitation of 1599 mm. The canopy height was 19 m and the LAI ranged from 4.5 to 5.5, with little fluctuation. The area around the observation tower tended to mildly incline at approximately 9.2°. The CO_2 concentration was measured at five heights (0.3, 1, 4, 14 and 20 m), and air temperature and relative humidity were measured at six heights (1, 4, 10, 14, 20 and 28 m). The measurement system and calculation method were almost the same as in this study. Reports by Ohkubo et al. (2007) and Ohkubo and Kosugi (2008) provide further details.

3. Results and discussion

3.1. Seasonal changes in storage fluxes

We calculated the mean diurnal changes in S_c, Q_a and Q_w by averaging all acquired data in every 30-min period for each month. During rain, we could obtain storage-flux data but not eddy-flux data because drops of water became attached to the lens of the IRGA probe (Li-7500). Figures 2–4 show the monthly mean diurnal changes in S_c, Q_a and Q_w, respectively. The plots show some scattering, which could be due to the small number of data (Table 1). As indicated in these figures, none of the storage fluxes showed large seasonal fluctuation. To investigate the seasonality of storage fluxes in detail, we compared the mean diurnal variations of storage fluxes with meteorological factors in the driest and wettest periods.

Figure 5 shows the mean diurnal variations of rainfall (a), solar radiation (b), air temperature at 53 m (c), vapour pressure deficit at 53 m (d), S_c (e), Q_a (f) and Q_w (g) in the driest and wettest periods during the observation. We selected the driest period data from days with the small volumetric soil water content (the daily average value from nine total sensors at 0.1, 0.2 and 0.3 m depths, <0.22 m^3 m^{-3}) during the dry season and the wettest period data from days with large volumetric soil water content (≥0.33 m^3 m^{-3}) during the rainy season. During the rainy season, it usually rained from afternoon until midnight. Rain and low solar radiation seldom occurred continuously all day long. Mean daily rainfall in the driest and wettest period were 0.9 and 12.7 (mm d^{-1}), respectively. Solar radiation values were similar in the early morning in the driest and wettest periods, but daily solar radiation in the wettest period (14.2 MJ d^{-1}) was smaller than that in the driest period (19.1 MJ d^{-1}). The diurnal amplitudes of air temperature and water vapour pressure deficit in the wettest period (5.6 °C and 7.3 hPa, respectively) were smaller than those in the driest period (7.3 °C and 8.9 hPa, respectively). The difference of air temperature and vapour pressure deficit

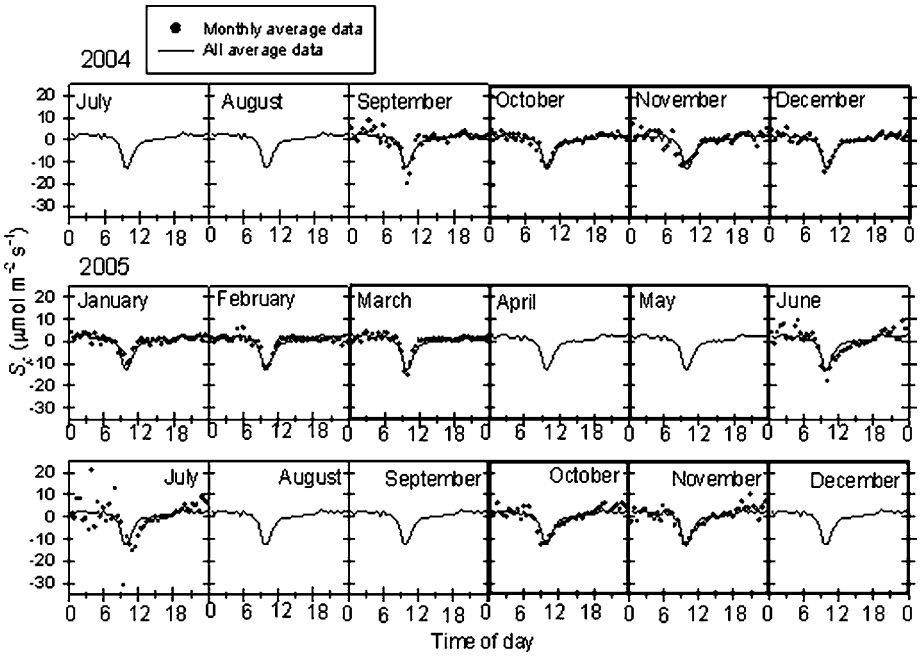

Fig. 2. Monthly ensemble averages of half-hourly values of S_c. Solid circles show the averaged value for each month, and the solid line indicates the averaged value for all available data. The rainy seasons (March to May and October to December) are enclosed by a thick line.

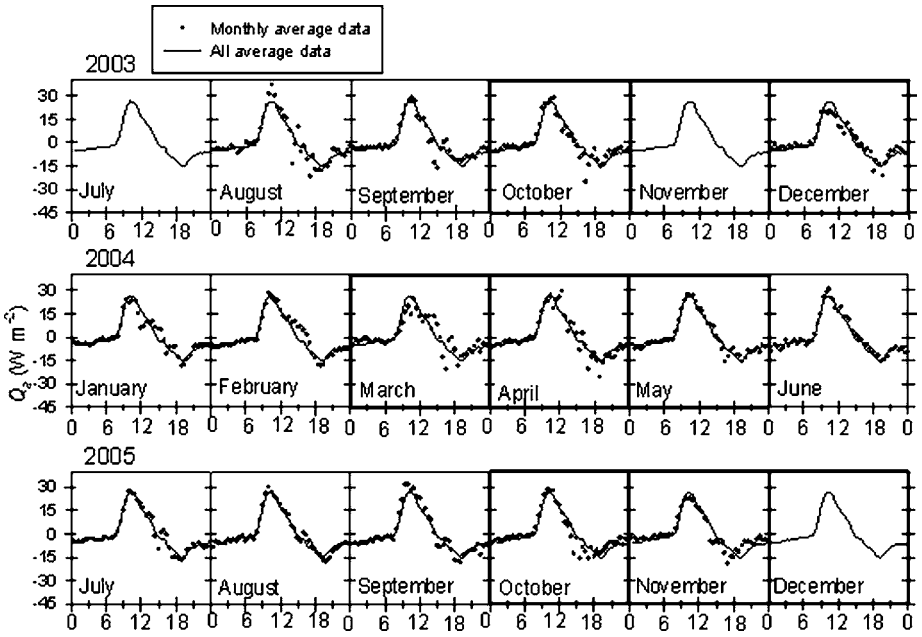

Fig. 3. Monthly ensemble averages of half-hourly values of Q_a. Solid circles show the averaged value for each month, and the solid line indicates the averaged value for all available data. The rainy seasons (March to May and October to December) are enclosed by a thick line.

between the wettest and driest periods became small in the early morning (0.7 °C and 1.3 hPa, respectively) and large in the afternoon (3.5 °C and 4.5 hPa, respectively).

Figure 5e shows that the negative peak of S_c in the wettest period was somewhat closer to zero than that in the driest period; this result may reflect the influence of a slightly smaller photosynthesis rate as a CO_2 sink due to the slightly smaller solar radiation in the wettest period (Fig. 5b). From sunset to midnight (19:00–24:00), the average S_c in the driest period (0.70 μmol m^{-2} s^{-1}) was smaller than that in the wettest period (2.92 μmol m^{-2} s^{-1}). This result corresponds to the nighttime F_c being slightly smaller under the driest condition (Kosugi et al.,

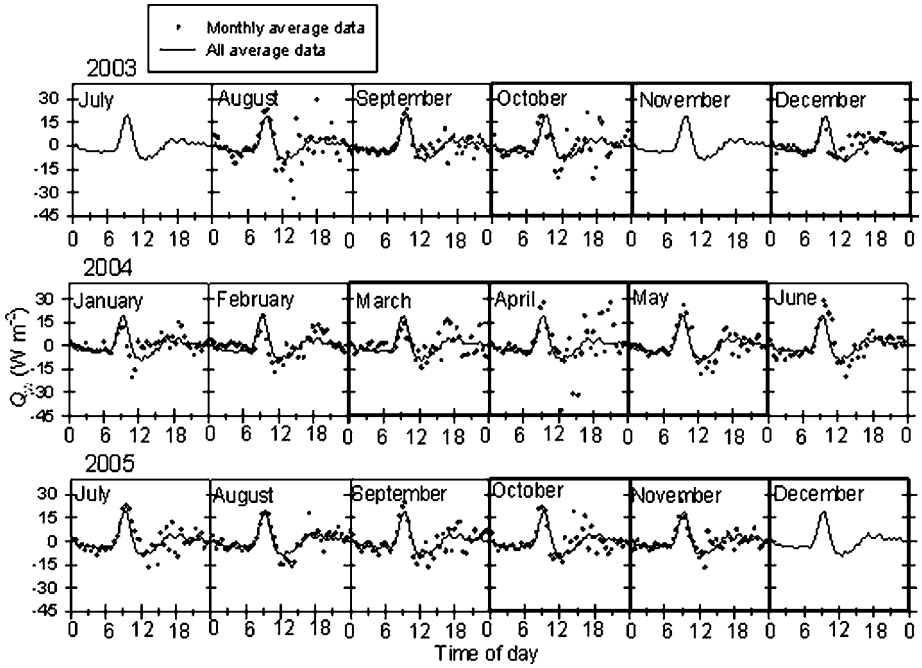

Fig. 4. Monthly ensemble averages of half-hourly values of Q_w. Solid circles show the averaged value for each month, and the solid line indicates the averaged value for all available data. The rainy seasons (March to May and October to December) are enclosed by a thick line.

2008). Kosugi et al. (2008) also reported that the soil respiration rate was low temporally, when the soil was dry. We can assume that the small nighttime S_c was due to the low soil respiration rate in the driest period, which contributed to nighttime ecosystem respiration as a CO_2 source.

In the case of Q_a, the positive peak in the morning, negative peak in the afternoon, and nighttime values in the wettest period were closer to zero than those in the driest period. The diurnal amplitude of Q_a in the wettest period (41.0 W m^{-2}) was smaller than that in the driest period (54.7 W m^{-2}; Fig. 5f), due to the lower solar radiation in the wettest period than in the driest period. On the other hand, no clear difference in the mean diurnal variation in Q_w was observed between the driest and wettest periods, although the plots scattered in the afternoon (Fig. 5g). These results correspond to the finding of no clear seasonal changes in $\lambda \boldsymbol{E}$, although $\boldsymbol{H}$ sometimes fluctuated between the dry and wet periods (Takanashi et al., unpublished).

3.2. Diurnal changes in vertical profiles and storage fluxes

3.2.1. Vertical CO_2 profiles and CO_2 storage fluxes (S_c). Figure 6 shows the mean diurnal variations in S_c, F_c and u_* (a) and the isoline of [CO_2] (b). The arrows indicate the average times of sunrise and sunset; solar noon was around 13:00 at this site. The diurnal variations shown in Fig. 6 were obtained by averaging all available data collected at 30-min intervals. From midnight to sunrise, [CO_2] increased at all heights with low u_* and was highest during the day at sunrise. After sunrise, [CO_2] rapidly decreased with increasing u_*, especially in the lower canopy, thereby reducing the vertical gradient. After 10:00, there was no clear vertical difference in [CO_2], and the concentrations throughout the forest were similar to those in the well-mixed atmosphere above the canopy space, except near the ground. From 13:00 to 18:00, [CO_2] throughout the canopy remained stable. In the afternoon, [CO_2] reached its minimum. Around 20:00, the vertical CO_2 gradient began to build again from the ground, and [CO_2] increased and became vertically stratified within the canopy. At the soil surface, [CO_2] was consistently higher than at any other level within the canopy. The S_c was greater than zero (2.2 μmol m^{-2} s^{-1} on average) at night (20:00–06:00) and dropped below zero after sunrise, whereas F_c remained positive. At 10:00, S_c reached its negative peak (-12.7 μmol m^{-2} s^{-1}), and F_c switched from positive to negative. At sunset, S_c and F_c both became positive. The average S_c over the daily cycle was 0.017 μmol m^{-2} s^{-1}, a value that was not significantly different from zero.

The diurnal vertical profiles of [CO_2] and S_c should be influenced by both air mixing and ecosystem processes. Two mechanisms can explain the rapid transition in [CO_2] after sunrise. First, much of the nocturnally stored CO_2 released during nighttime respiration may be rapidly reabsorbed by photosynthesis after sunrise, since the leaves are dispersed vertically below the canopy in this forest (i.e. there is no trunk space). This study site is located near the equator; so, solar altitude increases drastically and light can penetrate deeply into the canopy as time

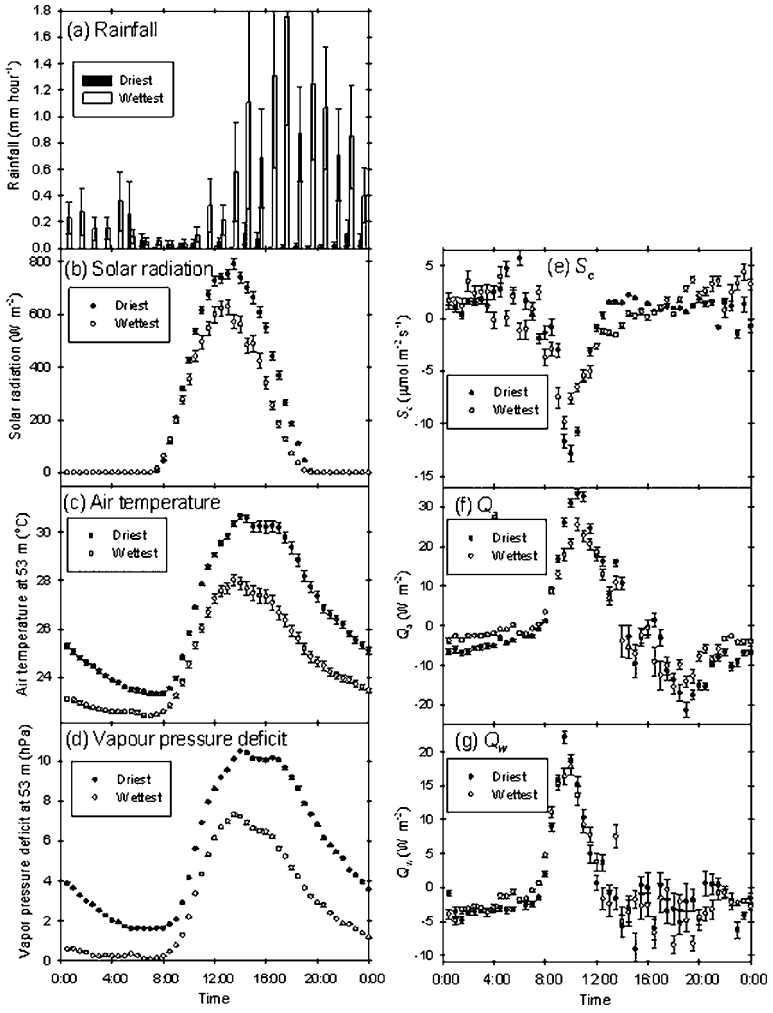

Fig. 5. Mean diurnal variations in rainfall (a), solar radiation (b), air temperature at 53 m (c), vapour pressure deficit at 53 m (d), S_c (e), Q_a (f) and Q_w (g) in the driest and wettest periods during the observation. The driest period data (black bars and solid circles) were selected from days with small volumetric soil water content (<0.22 m^3 m^{-3}, average value from nine total sensors at 0.1, 0.2 and 0.3 m depths) during the dry season, and the wettest period data (white bars and open circles) were selected from days with large volumetric soil water content (≥ 0.33 m^3 m^{-3}) during the rainy season. The error bars represent the standard errors of the means. The number of S_c values for the driest period and wettest period were 13 d (11% of available S_c data) and 23 d (20% of available S_c data), respectively. The numbers of Q_a and Q_w values in the driest period and wettest period were 36 d (11% of available Q_a and Q_w data) and 21 d (6% of available Q_a and Q_w data), respectively.

passes after sunrise. Because there is sufficient light soon after sunrise for photosynthesis to start, [CO_2] decreases rapidly. Second, the forest air is mixed and emitted upward from the canopy due to turbulence caused by heating of the air. Thus, u_* rapidly increased after sunrise (Fig. 6). At night, the elevated [CO_2] within the canopy was caused by the calm conditions, which trapped respired CO_2. After sunrise (around 7:00), [CO_2] at 10–30 m began to decrease due to photosynthetic activity. Thirty minutes later, [CO_2] at 0.2–5 m began to decrease. This time lag might have been due to tall trees and dense vegetation blocking light from reaching lower heights just after sunrise; thus, CO_2 emission from the soil may have strongly affected [CO_2] at lower heights. Then, [CO_2] at 45–53 m began to decrease. Two reasons might explain such a late decrease in [CO_2]. One is that there was no photosynthesis uptake above the canopy. The other is that [CO_2] below the canopy was still higher than [CO_2] above the canopy and increasing air mixing still increased [CO_2] above the canopy. For that reason, at 09:00, F_c was still positive whereas S_c was negative. This negative–positive difference implies that early-morning photosynthesis was not detected over the canopy by the eddy covariance measurement. The daytime [CO_2] was considerably lower than the nighttime [CO_2] because photosynthetic uptake of CO_2, which was greater than respiratory CO_2 emission and air mixing, occurred during the day, whereas respiratory efflux and accumulation of CO_2 by plants and soil occurred at night. The elevated [CO_2] near the forest floor suggests that gentle air mixing and soil respiration, which represent a large share of the respiration in the ecosystem, significantly influence this period. Larger amplitude has been found near the crown in tropical rainforests (e.g. Aoki et al., 1975; Kumagai et al., 2001), including at our site, than in other forest types (e.g. Brooks et al., 1997; Jarvis et al., 1997; Hollinger et al., 1998; Dolman et al., 2002; Kondo et al., 2005).

3.2.2. Vertical air temperature profiles and sensible heat storage fluxes (Q_a).

Figure 7 shows the mean diurnal variations in Q_a, $\boldsymbol{H}$ and u_* (a) and the air temperature isoline (b). At night, the air temperature decreased due to radiative cooling from the forest floor to the top of the canopy. At 07:30, the air temperature reached its minimum at every height; air temperature then reached its maximum at

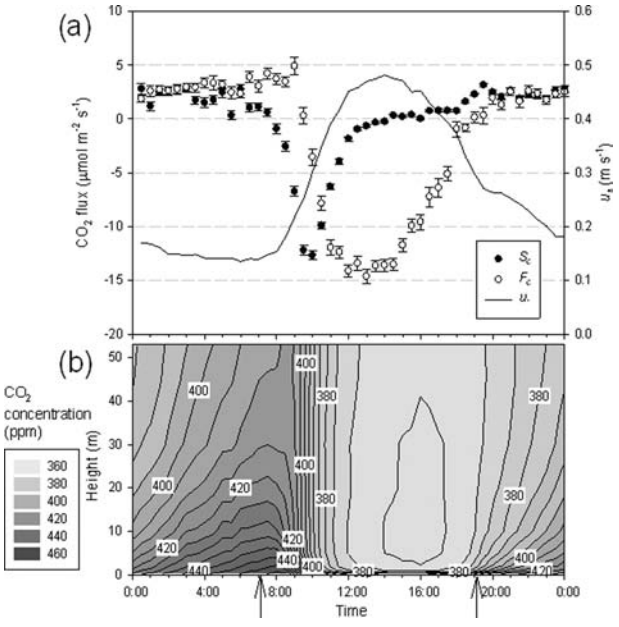

Fig. 6. (a) Mean diurnal variations in S_c (solid circles), F_c (open circles) and u_* (line), based on all available data (141 d). The error bars represent the standard errors of the means. (b) Isoline of the average CO_2 concentration distributions within the canopy as a function of height and time of day ($N = 141$ d). Isolines are indicated every 5 ppm. The arrows on the x-axis represent the average times of sunrise (ranging from 06:54 to 07:25) and sunset (ranging from 18:55 to 19:26) throughout the year.

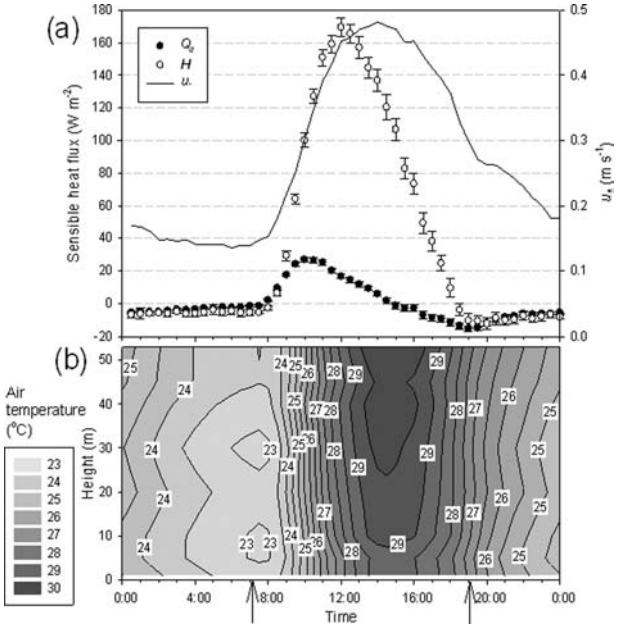

Fig. 7. (a) Mean diurnal variations in Q_a (solid circles), $\boldsymbol{H}$ (open circles) and u_* (line), based on all available data (336 d). The error bars represent the standard errors of the means. (b) Isoline of the average air temperature distributions within the canopy as a function of height and time of day ($N = 336$ d). Isolines are indicated every 0.5 °C. The arrows are as given in Fig. 6.

14:30 at all heights. The amplitude of the diurnal change in air temperature at 53 m (6.5 °C) was larger than that at 1 m (5.6 °C). The values of Q_a and $\boldsymbol{H}$ were negative at night but became positive after sunrise as the air temperature increased. This rapid increase after sunrise is due to light deeply entering the canopy, as discussed in the previous section. The positive peak of Q_a (27 W m^{-2}) occurred at 10:00, while $\boldsymbol{H}$ reached its positive peak (169 W m^{-2}) at noon. In the afternoon, Q_a dropped below zero as the air temperature decreased. Just before sunset, $\boldsymbol{H}$ also became negative, even as Q_a reached its negative peak (-15 W m^{-2}) at 19:00. The average Q_a over the daily cycle was 0.00029 W m^{-2}, a value that can be regarded as zero.

The deep penetration of light into the forest accounts for the amplitude difference in air temperature being small between the top (53 m) and bottom (1 m) of the forest. The diurnal pattern of Q_a (i.e. a positive peak for Q_a in the morning and negative peak in the afternoon) is similar to the patterns found at several other sites in various forest types (e.g. McCaughey and Saxton, 1988; Vogt et al., 1996; Silberstein et al., 2001; Turnipseed et al., 2002; Oliphant et al., 2004).

3.2.3. Vertical water vapour pressure profiles and latent heat storage fluxes (Q_w).

Figure 8 shows the mean diurnal variations in Q_w, $\lambda\boldsymbol{E}$ and u_* (a) and the average water vapour pressure isoline (b). The water vapour pressure decreased at all heights from midnight to sunrise, but increased rapidly after sunrise. Beginning at midday, the water vapour pressure decreased from 10:30 to 15:30, after which time it increased until midnight. This bimodal diurnal variation was observed everywhere except near the forest floor. The water vapour pressure near the forest floor was consistently higher than at any other level. Bimodal fluctuation was also found for Q_w due to the bimodal fluctuation in water vapour pressure. From 20:00 to 00:30, Q_w and $\lambda\boldsymbol{E}$ were both positive, while from 00:30 to 06:00, Q_w was negative and $\lambda\boldsymbol{E}$ was positive. After sunrise, Q_w became positive, peaking (20 W m^{-2}) at 09:30, while $\lambda\boldsymbol{E}$ reached its positive peak (250 W m^{-2}) at 13:00 and then decreased until again becoming positive in the evening. The average Q_w over the daily cycle was 0.014 W m^{-2}. Similarly to Q_a, this value can be considered zero.

Bimodal variation in Q_w depended on the $\delta e/\delta t$ at each height. Diurnal changes in the daytime water vapour pressure profile and Q_w were mainly controlled by the balance between the transpiration rate and the level of air mixing. The water vapour pressure increased from 07:30 at all levels because of the start of transpiration and low air mixing condition. It then decreased from 10:00 above the canopy (at 40–53 m), as the level of air mixing increased by the transport of water vapour upward from the canopy. Further decreases in the water vapour pressure were observed at 20–30 m from 10:30 and at 5–10 m from 11:00. The time lag reflects differences in the air mixing condition, which was weak at lower levels. In the afternoon, water vapour

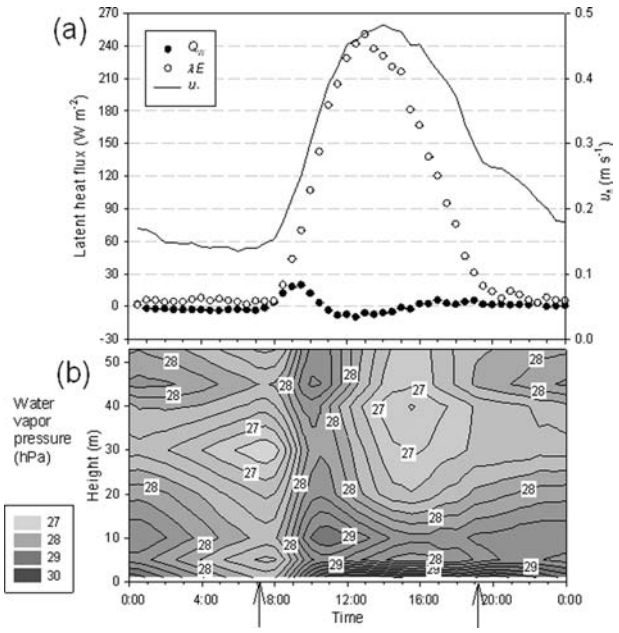

Fig. 8. (a) Mean diurnal variations in Q_w (solid circles), $\lambda \boldsymbol{E}$ (open circles) and u_* (line) based on all available data (336 d). The error bars represent the standard errors of the means. (b) Isoline of the average water vapour pressure distributions within the canopy as a function of height and time of day ($N = 336$ d). Isolines are indicated every 0.25 hPa. The arrows are as given in Fig. 6.

pressure except at 1 m started to increase due to decreasing u_*. After sunset, the evapotranspiration rate dropped, and water vapour pressure at 1 m began to decrease. At 1 m, air mixing was weak all day long, and the evapotranspiration rate mainly controlled the water vapour pressure.

Oliphant et al. (2004) also reported two positive peaks in the diurnal profile of Q_w in a temperate deciduous forest in summer. On the other hand, Q_w showed no clear bimodal diurnal variation at other sites (e.g. McCaughey and Saxton, 1988; Vogt et al., 1996; Silberstein et al., 2001; Turnipseed et al., 2002). The differences may be due to the smaller number of levels (e.g. three) and shorter observation periods used in those studies.

3.3. *Differences in the storage fluxes under various meteorological conditions*

Turbulent mixing and the source/sink intensity (i.e. respiration and photosynthesis, in the case of CO_2) govern the dynamics of CO_2 within a forest canopy (Brooks et al., 1997). These factors also govern the dynamics of sensible and latent heat storage fluxes. Solar radiation strongly influences photosynthesis and transpiration; therefore, solar radiation is a good index of the sources/sinks of CO_2, sensible heat and latent heat. Solar radiation also makes up a large part of the net radiation and is thus the main energy source for heat fluxes. We investigated how u_*, which is an index of turbulent mixing, and solar radiation influenced the storage fluxes S_c, Q_a and Q_w at this site.

Figure 9 shows the transition of S_c, Q_a and Q_w with u_* in panels I, II and III, respectively. Ensemble-averaged storage fluxes and eddy fluxes for each u_* range during the day and at night are shown in panels (a) and (b), respectively. The ensemble mean diurnal variations in the vertical $[CO_2]$ profile were classified into two patterns based on the average u_* at night (Fig. 10). Similarly, the ensemble mean diurnal variations in S_c and F_c (a), Q_a and $\boldsymbol{H}$ (b) and Q_w and $\lambda \boldsymbol{E}$ (c) were classified into two patterns by the daily accumulated solar radiation patterns (Fig. 11).

Figure 9I-a, shows that the negative value of S_c approached zero as u_* increased during the day, whereas F_c decreased except when the range of u_* was very low. On the other hand, panel I-b shows that the positive value of S_c approached zero as u_* increased at night, whereas F_c increased. At night, CO_2 is emitted throughout the forest and turbulence with a high u_* value accelerates the upward emission of CO_2 from the canopy. This leads to a decrease in S_c and an increase in F_c with increasing u_* (Fig. 9I-b). As shown in Fig. 10, when the nighttime u_* was high, $[CO_2]$ was lower than that at low u_*, especially at the lower levels. In daytime, there were no clear differences between the two accumulated daily solar radiation patterns of S_c, although the negative peak of S_c with small solar radiation was slightly closer to zero than that with large solar radiation (Fig. 11a). At this site, canopy photosynthesis and stomatal conductance did not differ between sunny and cloudy days and showed an obvious trend of decline from late morning and in the afternoon, irrespective of whether it was a sunny or cloudy day or the rainy or dry season (Takanashi et al., 2006; Kosugi et al., 2008). Thus, differences in solar radiation at this site had no obvious influence on either F_c or S_c.

Panels II-a and III-a of Fig. 9 show that Q_a and Q_w decreased with increasing u_* during the day, in contrast to the increases in $\boldsymbol{H}$ and $\lambda \boldsymbol{E}$, whereas panels II-b and III-b of Fig. 9 demonstrate that at night Q_a and Q_w were not obviously influenced by u_*. During the day, as u_* increased, Q_a and Q_w decreased while $\boldsymbol{H}$ and $\lambda \boldsymbol{E}$ increased because the turbulence above the canopy promoted the release of heat and water stored in the forest. Values of Q_a and Q_w were unaffected by increases in u_* at night, when there were no notable sinks or sources; thus vertical gradients of air temperature and water vapour pressure did not form. The diurnal amplitudes of Q_a and Q_w with larger solar radiation were larger than those with smaller solar radiation (Figs. 11b and c).

These results indicate that air mixing at night controlled the large contribution of S_c to the exchange of CO_2 between the forest and the atmosphere but did not greatly influence Q_a and Q_w. On the other hand, larger solar radiation led to larger diurnal amplitudes of Q_a and Q_w, but did not largely influence S_c. This difference in daytime coincided with that of eddy covariance fluxes measured over the canopy.

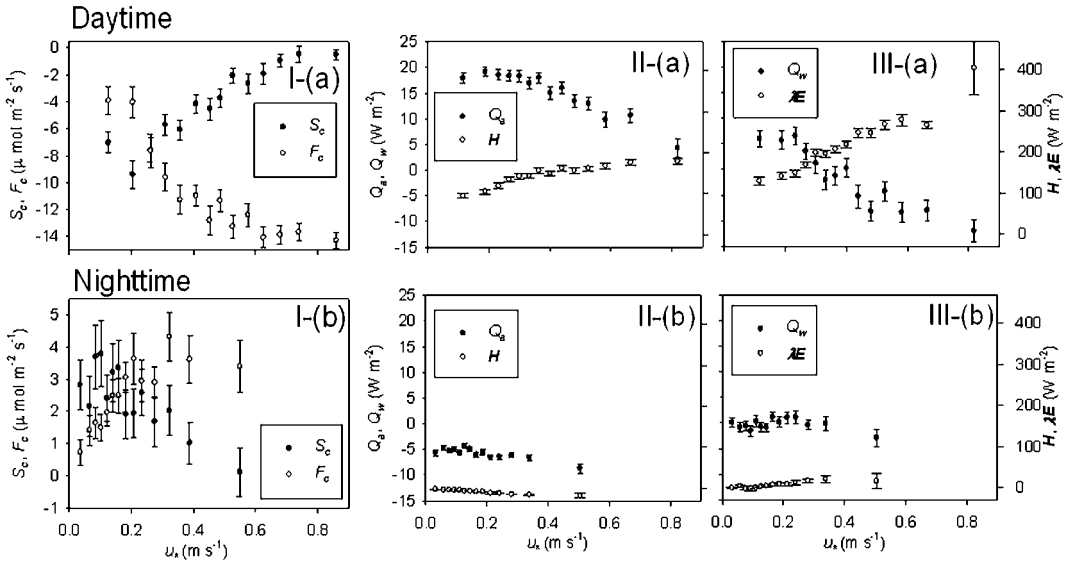

Fig. 9. Storage fluxes S_c (I), Q_a (II) and Q_w (III) (solid circles) and eddy fluxes F_c (I), $\boldsymbol{H}$ (II) and $\lambda\boldsymbol{E}$ (III) (open circles) for each u_* range. The upper panels show daytime (09:00–15:00) data (a) and the lower panels show nighttime (21:00–03:00) data (b). The error bars represent the standard errors of the means.

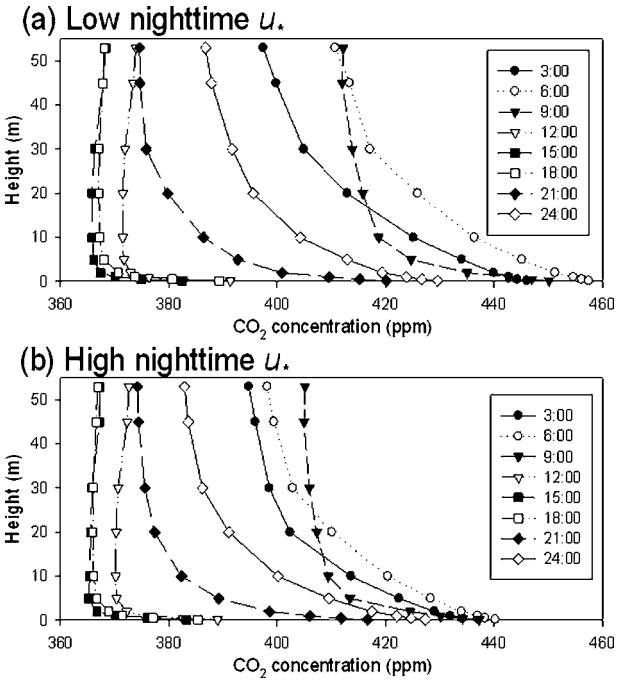

Fig. 10. Mean diurnal variations in the vertical profiles of the CO_2 concentration for two nighttime u_* patterns. We classified the patterns by the average u_* at night (00:00–06:00) into (a) <0.15 m s^{-1} versus (b) ≥0.15 m s^{-1}. The number of data points in (a) and (b) are 40 and 50, respectively. The [CO_2] profiles are based on measurements taken every 3 h.

3.4. *Contribution of storage fluxes to the exchange of CO_2 and energy*

Although storage fluxes (especially Q_a and Q_w) had a diurnal mean close to zero, they could contribute significantly to the exchange of CO_2 and energy on a half-hourly basis. The negative peak of the mean diurnal change in S_c (-12.7 μmol m^{-2} s^{-1}) corresponded to 86% of the negative peak of F_c (Fig. 6). Figure 6a shows that the nighttime respiratory efflux of CO_2 from the forest floor and the standing biomass were considerably underestimated by F_c alone. On average, the nocturnal (i.e. 20:00–06:00) value of S_c (2.2 μmol m^{-2} s^{-1}) was roughly half of the value of $F_c + S_c$ (4.7 μmol m^{-2} s^{-1}). The contribution ratio of S_c to $F_c + S_c$ ranged from -419 to 370%. The contribution became large when $F_c + S_c$ approached zero just after sunrise and before sunset. After sunrise, the contribution ratio of S_c to $F_c + S_c$ decreased with increasing $F_c + S_c$ and eventually became nearly zero.

The positive peaks of Q_a (27 W m^{-2}) and Q_w (20 W m^{-2}) were 16 and 7.8% of the positive peaks of $\boldsymbol{H}$ and $\lambda\boldsymbol{E}$, respectively (Figs. 7 and 8). The contribution ratios of Q_a and Q_w to $\boldsymbol{H} + \lambda\boldsymbol{E} + Q_a + Q_w$ ranged from -152 to 273% and -33 to 90%, respectively, and the contribution became large when $\boldsymbol{H} + \lambda\boldsymbol{E} + Q_a + Q_w$ was small during nighttime. Contributions of Q_a and Q_w were about half of $\boldsymbol{H} + \lambda\boldsymbol{E} + Q_a + Q_w$ from midnight to sunrise. After sunrise, the contribution ratios of Q_a and Q_w decreased with increasing $\boldsymbol{H} + \lambda\boldsymbol{E} + Q_a + Q_w$ and approached zero. Wilson et al. (2002) reported that the energy balance

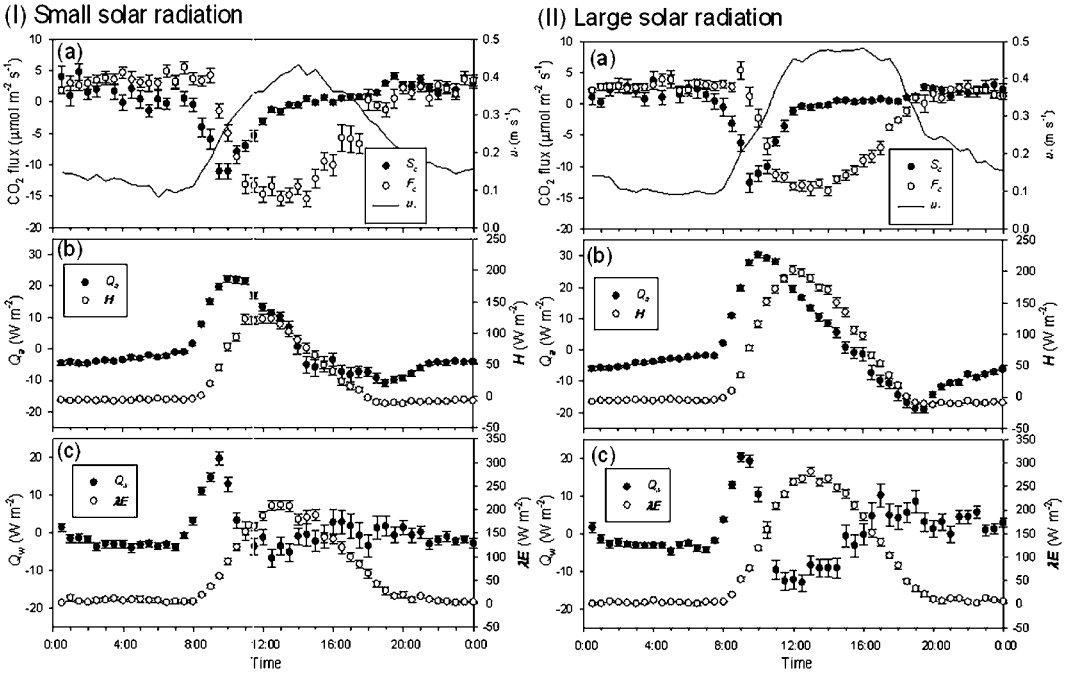

Fig. 11. Mean diurnal variations in u_* and the storage fluxes (S_c, F_c, Q_a, $\boldsymbol{H}$, Q_w and $\lambda\boldsymbol{E}$) for two daily accumulated solar radiation patterns. Using the solar radiation, we classified the values into patterns I (< 17 MJ d^{-1}) and II (≥ 17 MJ d^{-1}). There were 125 and 170 values in classifications I and II, respectively. (a) Mean diurnal variations in u_* (solid line), S_c (solid circles) and F_c (open circles). (b) Mean diurnal variations in Q_a (solid circles) and $\boldsymbol{H}$ (open circles). (c) Mean diurnal variations in Q_w (solid circles) and $\lambda\boldsymbol{E}$ (open circles). The error bars represent the standard errors of the means.

ratio during nighttime was smaller than that in daytime and that a weak air mixing condition decreased the energy balance ratio. Our results indicate that the contributions of Q_a and Q_w to $\boldsymbol{H} + \lambda\boldsymbol{E} + Q_a + Q_w$ were large during nighttime, and Q_a and Q_w became larger with smaller u_* (Fig. 9). We can assume that Q_a and Q_w are quite important when the energy balance ratio is small, and that other components such as advection would also largely influence the energy balance under such a condition.

To reveal which factors influence the storage fluxes and how, we compared our data from PSO in a tropical rainforest with summertime data from Kiryu Experimental Watershed (KEW) in a temperate Japanese cypress forest (Ohkubo et al., 2007; Ohkubo and Kosugi, 2008). Canopy height at PSO was about twice that at KEW. The LAI at PSO was also slightly larger than that at KEW. Leaves were distributed vertically at PSO whereas the KEW forest had a dense crown and trunk space. Further, KEW was mainly covered by *Chamaecyparis obtusa* Sieb. et Zucc. (Japanese cypress, an evergreen conifer), whereas PSO was covered by a primary forest of lowland mixed dipterocarp (tropical evergreen broadleaved forest), which included various species of *Shorea* and *Dipterocarpus*. The observation system and calculation method for storage fluxes were almost the same at both sites. Thus, we could neglect methodological differences between these two study sites.

Figure 12 presents comparisons of the diurnal variation of the air temperature and water vapour deficit (a), u_* and solar radiation (b), S_c and F_c (c), Q_a and $\boldsymbol{H}$ (d) and Q_w and $\lambda\boldsymbol{E}$ (e) at PSO to those at KEW in summer. Solar noon at PSO was about 1 h later than that at KEW. Air temperatures and water vapour deficit were almost the same at the two sites, ranging from 23.0 to 29.0 °C and 1.1 to 11.4 hPa at KEW and 23.2 to 28.7 °C and 0.7 to 9.7 hPa at PSO, respectively (Fig. 12a). At PSO, u_* was smaller especially during night and early morning and solar radiation was slightly larger than at KEW (Fig. 12b). During nighttime, average S_c from 20:00 to 06:00 at PSO (2.2 μmol m^{-2} s^{-1}) was larger than that from 20:00 to 04:00 at KEW (0.8 μmol m^{-2} s^{-1}; Fig. 12c). The diurnal amplitude of S_c at PSO (15.9 μmol m^{-2} s^{-1}) was about three times larger than that at KEW (4.8 μmol m^{-2} s^{-1}), whereas the diurnal amplitudes of Q_a and Q_w at PSO (42 W m^{-2} and 30 W m^{-2}) were also larger than those at KEW (30 W m^{-2} and 14 W m^{-2}; Figs. 12d and e). The diurnal variations of F_c, $\boldsymbol{H}$ and $\lambda\boldsymbol{E}$ at KEW were similar to those at PSO, although F_c at PSO was slightly smaller than that at KEW.

We assumed that the differences in u_* during nighttime mainly reflected differences in S_c between the two sites, because CO_2 emitted by ecosystem respiration would be easily stored under the condition of weak air mixing (low u_*). Negative S_c would also become larger because a large amount of stored CO_2 would be released upward from the canopy before sunrise. Meanwhile,

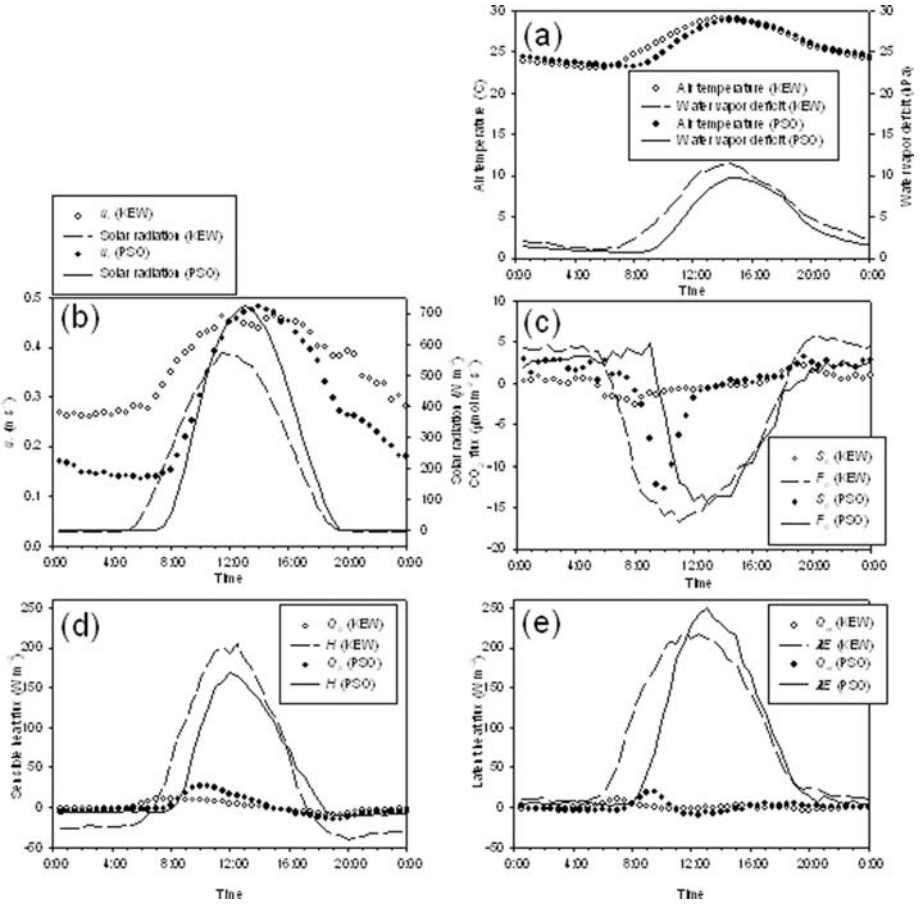

Fig. 12. (a) Diurnal variation in air temperature and water vapour pressure at Kiryu Experimental Watershed (KEW) in a temperate Japanese cypress forest (Ohkubo and Kosugi, 2008; open circles and dashed line) and at the present study site at Pasoh Forest Reserve (PSO) in a tropical rainforest (solid circles and thick line). (b) Diurnal variation in u_* and solar radiation at KEW (open circles and dashed line) and at PSO (solid circles and thick line). (c) Diurnal variation in S_c and F_c at KEW (open circles and dashed line) and at PSO (solid circles and thick line). (d) Diurnal variation in Q_a and $\boldsymbol{H}$ at KEW (open circles and dashed line) and at PSO (solid circles and thick line). (e) Diurnal variation in Q_w and $\lambda\boldsymbol{E}$ at KEW (open circles and dashed line) and at PSO (solid circles and thick line).

the strength of u_* did not seem to have much influence on Q_a and Q_w at night, because sink/source intensity was smaller in the cases of heat and water vapour compared with CO_2.

As also shown in Fig. 12, PSO and KEW had similar nighttime $F_c + S_c$ values in summer. However, we expect that nighttime ecosystem respiration at PSO was larger than that at KEW and that the larger source of CO_2 also somewhat influenced the larger S_c at PSO. Ohkubo et al. (2007) reported that nocturnal $F_c + S_c$ was nearly equal to total ecosystem respiration with high u_* at KEW, whereas Kosugi et al. (2008) reported that $F_c + S_c$ corresponded only to the component of soil respiration estimated with the chamber method, even at a moderate friction velocity ($u_* > 0.2$ m s^{-1}). We can assume that our $F_c + S_c$ data considerably underestimated nighttime ecosystem respiration at PSO even under moderate u_*, and thus, the actual mean nighttime CO_2 source, as the ecosystem respiration was likely greater than the nocturnal value of $F_c + S_c$.

Next, we compared nighttime ecosystem respiration as a CO_2 source between KEW in summer and PSO. Using the average from June to August for two summers (2003–2004), Ohkubo et al. (2007) estimated the summertime soil respiration rate at KEW to be 3.1 μmol m^{-2} s^{-1}, which represented 49.6% of the total ecosystem respiration (6.2 μmol m^{-2} s^{-1}). Kosugi et al. (2008) estimated the average soil respiration rate at PSO for 3 yr (2003–2005) to be 4.1 μmol m^{-2} s^{-1}. Total ecosystem respiration includes respiration from stem, foliage and coarse surface litter components other than soil respiration (root respiration, fine surface litter and soil organic matter decomposition) and is likely to be greater than soil respiration. The above estimates for ecosystem respiration at the two sites are consistent with the findings that $F_c + S_c$ underestimated ecosystem respiration at PSO, and that the $F_c + S_c$ values were similar at the two sites. In addition to the weak air mixing condition, a larger CO_2 source would make S_c somewhat large at PSO. The

underestimation would be caused by advection over non-flat terrain with relatively small u_* compared with other forest types.

Comparison of S_c values at our study site and other forests revealed larger S_c in tropical forests than in other forest types (e.g. Jarvis et al., 1997; Hollinger et al., 1998; Dolman et al., 2002). Further, the S_c found for a central Amazonian forest (Malhi et al., 1998) was as large as that for our tropical rainforest site. We also compared Q_a and Q_w with those at other study sites (e.g. McCaughey and Saxton, 1988; Vogt et al., 1996; Silberstein et al., 2001; Turnipseed et al., 2002; Oliphant et al., 2004) but could not find clear differences between our site and other sites. This result could reflect methodological differences and the shorter observation periods in most past studies. However, we could also assume that there are no conspicuous differences in Q_a and Q_w between various forest types, unlike for S_c. The difference in S_c characteristics between two tropical rainforest sites might be caused by a combination of weaker air mixing and a larger source. On the other hand, the small differences of Q_a and Q_w would be due to the small sinks/sources of heat and water vapour among these forest sites at night.

4. Conclusions

Using 3 yr (2003–2005) of intermittent observations of $[CO_2]$, air temperature and relative humidity at several heights from the floor to the canopy top of a tropical rainforest at Pasoh, Peninsular Malaysia, we analysed the amplitude and diurnal profiles of $[CO_2]$, air temperature and water vapour pressure as well as S_c, Q_a and Q_w and their contributions to CO_2 and energy exchanges. From sunset to midnight, S_c in the driest period was slightly smaller than that in the wettest period. This result corresponds to the finding that nighttime F_c was slightly smaller under the driest condition (Kosugi et al., 2008), reflecting the low soil respiration rate in the dry period, which largely contributed to nighttime ecosystem respiration as a CO_2 source. The diurnal amplitude of Q_a in the wettest period was slightly smaller than that in the driest period. However, no clear difference was found for Q_w. These results correspond to the finding of no clear seasonal changes in $\lambda \boldsymbol{E}$, while $\boldsymbol{H}$ sometimes fluctuated between the dry and wet periods (Takanashi et al., unpublished). The small fluctuation of Q_a can be explained by the low solar radiation in the wet period.

At night, S_c contributed to the CO_2 exchange between the forest and the atmosphere, being greater under low u_* conditions than under high u_*. In contrast, the strength of air mixing (u_*) at night did not heavily influence Q_a and Q_w. In daytime, Q_a and Q_w had larger diurnal amplitudes when solar radiation was greater; in contrast, the diurnal variation of S_c did not depend greatly on solar radiation. Comparison of our data with summertime data from a temperate Japanese cypress forest suggested a much higher contribution of S_c at our tropical rainforest study site, mainly because of lower nighttime u_*. Weak air mixing would make S_c large. Further comparison with other forest sites indicated that the weak air mixing condition at our site also created a vertical gradient of CO_2, air temperature and water vapour pressure within the forest. Such a situation could induce a time lag in the diurnal variation of these meteorological factors, depending on the height from the ground. The larger source from ecosystem respiration at this site would also make S_c somewhat large. On the other hand, differences in Q_a and Q_w were smaller than the difference in S_c among sites, probably because of the lack of sizable heat and water vapour sources at nighttime. Our long-term observations revealed that the diurnal patterns of each storage flux form from a combination of the strength of air mixing (u_*) and the availability of sources and sinks.

5. Acknowledgments

We thank the Forestry Department of Negeri Sembilan and the Director General of the Forest Research Institute Malaysia (FRIM) for permitting us to work in the Pasoh Forest Reserve. We also thank the staff of the Hydrology Unit and the Pasoh Station of the FRIM for collecting data. Dr. Kaoru Niiyama provided the LAI data for the forest reserve. We also thank Dr. Toshinori Okuda, Dr. Naishen Liang and the members of a joint research project between FRIM, Universiti Putra Malaysia and the National Institute for Environmental Studies, Japan, for assisting with our fieldwork. This study was supported by the Global Environment Research Fund of the Japan Environment Agency and by scientific research grants from the Ministry of Education, Culture, Sports, Science, and Technology, Japan and also by Grants-in-Aid for Scientific Research from the Japan Society for the Promotion of Science.

References

Aoki, M., Yabuki, K. and Koyama, H. 1975. Micrometeorology and assessment of primary production of a tropical rain forest in West Malaysia. *J. Agric. Met.* **31**, 115–124.

Baldocchi, D. 2003. Assessing the eddy covariance technique for evaluating carbon dioxide exchange rates of ecosystems: past, present and future. *Global Change Biol.* **9**, 479–492.

Brooks, J. R., Flanagan, L. B., Varney, G. T. and Ehleringer, J. R. 1997. Vertical gradients in photosynthetic gas exchange characteristics and refixation of respired CO_2 within boreal forest canopies. *Tree Physiol.* **17**, 1–12.

Dolman, A. J., Moors, E. J. and Elbers, J. A. 2002. The carbon uptake of a mid-latitude pine forest growing on sandy soil. *Agric. For. Meteorol.* **111**, 157–170.

Feigenwinter, C., Bernhofer, C., Eichelmann, U., Heinesch, B., Hertel, M. and co-authors. 2008. Comparison of horizontal and vertical advective CO_2 fluxes at three forest sites. *Agric. For. Meteorol.* **148**, 12–24.

Finnigan, J. J. 2006. The storage term in eddy flux calculations. *Agric. For. Meteorol.* **136**, 108–113.

Hollinger, D. Y., Kelliher, F. M., Schulze, E.-D., Bauer, G., Arneth, A. and co-authors. 1998. Forest-atmosphere carbon dioxide exchange in eastern Siberia. *Agric. For. Meteorol.* **90**, 291–306.

Jarvis, P. G., Massheder, J. M., Hale, S. E., Moncrieff, J. B., Rayment, M. and co-authors. 1997. Seasonal variation of carbon dioxide, water vapor, and energy exchange of a boreal black spruce forest. *J. Geophys. Res.* **102**, 28 953–28 966.

Kondo, M., Muraoka, H., Uchida, M., Yazaki, Y. and Koizumi, H. 2005. Refixation of respired CO_2 by understory vegetation in a cool-temperate deciduous forest in Japan. *Agric. For. Meteorol.* **134**, 110–121.

Kosugi, Y., Takanashi, S., Ohkubo, S., Matsuo, N., Tani, M. and co-authors. 2008. CO_2 exchange of a tropical rain forest at Pasoh in Peninsular Malaysia. *Agric. For. Meteorol.* **148**, 439–452.

Kumagai, T., Kuraji, K., Noguchi, H., Tanaka, Y., Tanaka, K. and co-authors. 2001. Vertical profiles of environmental factors within tropical rainforest. *J. For. Res.* **6**, 257–264.

Lamaud, E., Ogée, J., Brunet, Y. and Berbigier, P. 2001. Validation of eddy flux measurements above the understorey of a pine forest. *Agric. For. Meteorol.* **106**, 187–203.

Law, B. E., Ryan, M. G. and Anthoni, P. M. 1999. Seasonal and annual respiration of a ponderosa pine ecosystem. *Global Change Biol.* **5**, 169–182.

Lee, X. 1998. On micrometeorological observations of surface–air exchange over tall vegetation. *Agric. For. Meteorol.* 91, 39–49.

Malhi, Y., Nobre, A. D., Grace, J., Kruijt, B., Pereira, M. G. P. and co-authors. 1998. Carbon dioxide transfer over a Central Amazonian rain forest. *J. Geophys. Res.* **103**, 31 593–31 612.

McCaughey, J. H. and Saxton, E. L. 1988. Energy balance storage terms in a mixed forest. *Agric. For. Meteorol.* **44**, 1–18.

Mölder, M., Lindroth, A. and Halldin, S. 2000. Water vapor, CO_2, and temperature profiles in and above a forest-accuracy assessment of an unattended measurement system. *J. Atmos. Ocean. Technol.* **17**, 417–425.

Noguchi, S., Nik, A. R. and Tani, M. 2003. Rainfall characteristics of tropical rainforest at Pasoh Forest Reserve, Negeri Sembilan, Peninsular Malaysia. In: *Pasoh: Ecology of a Lowland Rain Forest in Southeast Asia*, (eds T. Okuda, N. Manokaran, Y. Matsumoto, K. Niiyama, S. C. Thomas and P. S. Ashton), Springer, Tokyo, 51–58.

Ohkubo, S. and Kosugi, Y. 2008. Amplitude and seasonality of storage fluxes for CO_2, heat and water vapor in a temperate Japanese cypress forest. *Tellus* **60B**, 11–20.

Ohkubo, S., Kosugi, Y., Takanashi, S., Mitani, T. and Tani, M. 2007. Comparison of the eddy covariance and automated closed chamber methods for evaluating nocturnal CO_2 exchange in a Japanese cypress forest. *Agric. For. Meteorol.* **142**, 50–65.

Oliphant, A. J., Grimmond, C. S. B., Zutter, H. N., Schmid, H. P., Su, H.-B. and co-authors. 2004. Heat storage and energy balance fluxes for a temperate deciduous forest. *Agr. For. Meteorol.* **126**, 185–201.

Silberstein, R., Held, A., Hatton, T., Viney, N. and Sivapalan, M. 2001. Energy balance of a natural jarrah (*Eucalyptus marginata*) forest in Western Australia: measurements during the spring and summer. *Agric. For. Meteorol.* **109**, 79–104.

Sun, J., Burns, S., Delaney, A., Oncley, S., Turnipseed, A. and co-authors. 2007. CO_2 transport over complex terrain. *Agric. For. Meteorol.* **145**, 1–21.

Takanashi S., Kosugi, Y., Matsuo, N., Tani, M. and Ohte, N. 2006. Patchy stomatal behavior in broad-leaved trees grown in different habitats. *Tree Physiol.* **26**, 1565–1578.

Turnipseed, A. A., Blanken, P. D., Anderson, D. E. and Monson, R. K. 2002. Energy budget above a high-elevation subalpine forest in complex topography. *Agric. For. Meteorol.* **110**, 177–201.

Vogt, R., Bernhofer, Ch., Gay, L. W., Jaeger, L. and Parlow, E. 1996. The available energy over a Scots pine plantation: what's up for partitioning? *Theor. Appl. Climatol.* **53**, 23–31.

Webb, E. K., Pearman, G. I. and Leuning, R. 1980. Correction of flux measurements for density effects due to heat and water vapour transfer. *Quart. J. R. Met. Soc.* **106**, 85–100.

Wilson, K. B., Goldstein, A., Falge, E., Aubinet, M., Baldocchi, D. and co-authors. 2002. Energy balance closure at FLUXNET sites. *Agric. For. Meteorol.* **113**, 223–243.

Xu, L.-K., Matista, A. A. and Hsiao, T. C. 1999. A technique for measuring CO_2 and water vapor profiles within and above plant canopies over short periods. *Agric. For. Meteorol.* **94**, 1–12.

Yasuda, Y., Ohtani, Y., Watanabe, T., Okano, M., Yokota, T. and co-authors. 2003. Measurement of CO_2 flux above a tropical rain forest at Pasoh in Peninsular Malaysia. *Agric. For. Meteorol.* **114**, 235–244.